33rd Annual International Conference of the IEEE EMBS
Boston, Massachusetts USA, August 30 - September 3, 2011

Optimal Tracking of a sEMG based Force Model for a Prosthetic Hand

Chandrasekhar Potluri, *Member, IEEE*, Madhavi Anugolu, *Member, IEEE*, YimeskerYihun, Alex Jensen, Steve Chiu, *Member, IEEE*, Marco P. Schoen, *Senior Member, IEEE*, and D. Subbaram Naidu, *Fellow, IEEE*.

***Abstract*: This paper presents a surface electromyographic (sEMG)-based, optimal control strategy for a prosthetic hand. System Identification (SI) is used to obtain the dynamic relation between the sEMG and the corresponding skeletal muscle force. The input sEMG signal is preprocessed using a Half-Gaussian filter and fed to a fusion-based Multiple Input Single Output (MISO) skeletal muscle force model. This MISO system model provides the estimated finger forces to be produced as input to the prosthetic hand. Optimal tracking method has been applied to track the estimated force profile of the Fusion based sEMG-force model. The simulation results show good agreement between reference force profile and the actual force.**

I. Introduction

Currently there are more than 2 million Americans that have a missing limb. The number of Americans with missing limbs increases 185,000 people a year [1]. As a result of this rising number of people that need prostheses, research is being focused on creating more intuitive prosthetics. There has been active research to design a prosthetic hand. But even today there is no prosthetic hand at an affordable cost with position and tactile force control [2]. It is evident from the past research that the human-centered robotics should be autonomous with a high level of functionality, comfort and ease of use [3]. A natural means of communication is required for human-centered robotics [4], and in the case of electromyographic (EMG) based prostheses, one natural means of interface between the human arm and prosthesis is the surface EMG (sEMG) itself. The EMG signal is present because of the neuromuscular activity in the body. The sEMG signals are captured noninvasively and give access to physiological processes responsible for the contraction of muscles. Since the sEMG signal is amplitude modulated and time dependent, and dynamic in nature, spatially and temporally frequency encoded [5]. Usually sEMG measurements are based on single sensor data. For this work we used an array of three sEMG sensors and a force sensing resistor (FSR) to acquire the EMG signal and the corresponding skeletal muscle force. The data from the three sEMG sensors are fused using a fusion algorithm to have a better estimation of skeletal muscle force from the corresponding sEMG signal when compared to single sensor data [6].

Chandrasekhar Potluri is with Measurement and Control Engineering Research Center (MCERC), College of Engineering, Idaho State University, Pocatello, Idaho 83209, USA (e-mail: potlchan@isu.edu).

Madhavi Anugolu is with MCERC, College of Engineering, Idaho State University, Pocatello, Idaho 83209, USA (email: anugmadh@isu.edu).

YimeskerYihun is with MCERC, College of Engineering, Idaho State University, Pocatello, Idaho 83209, USA (email: yihuyime@isu.edu).

Alex Jensen is with MCERC;is with MCERC, College of Engineering, Idaho State University, Pocatello, Idaho 83209, USA (email:jensalex@isu.edu)

Steve Chiu is with Department of Electrical Engineering and Computer Science, MCERC, Idaho State University, Pocatello, Idaho 83209 USA (email: chiustev@isu.edu).

Marco P. Schoen is with Department of Mechanical Engineering, MCERC, Idaho State University, Pocatello, Idaho 83209, USA (email: schomarc@isu.edu).

D. Subbaram Naidu is with Department of Electrical Engineering and Computer Science, MCERC, Idaho State University, Pocatello, Idaho 83209 USA (email: naiduds@isu.edu).

This paper uses the sEMG-force fusion model as reference profile. A Linear Quadratic Tracking (LQT) technique is employed to the prosthetic hand to track the force profile. This paper is structured as follows. The experimental set up is given in Section II, Section III provides reference force model and Section V provides dynamics of the hand. Section VI details the results and discussion and in the last section some conclusions are provided.

II. Experimental Set-Up

Experiments were conducted on a right-handed healthy male subject. Using a muscle simulator (Rich-Mar Corporation HV 1100), motor units were marked and sEMG sensors were placed accordingly [6]. One sEMG sensor was placed on the motor point of the subject's ring finger and two sensors were placed at points adjacent to it. Prior to placing the sEMG sensors, the skin surface of the subject was prepared according to International Society of Electrophysiology and Kinesiology (ISEK) protocols [7]. Both sEMG and muscle force signals were acquired simultaneously using LabVIEW™ 8.2 at a sampling rate of 2000 Hz. The sEMG data was captured by a DELSYS® Bagnoli-16 EMG system with DE-2.1 differential EMG sensors. The force information was collected by a NI ELVIS with an Interlink Electronics FSR 0.5" circular force sensor.

III. Reference Force Model

In this present work the force signal is extracted from the sEMG signals obtained from the array of the three sEMG sensors located on the arm. The data from the three sensors are collected around the corresponding individual motor unit location at the transradial arm location (flexor digitorum superficialis) and is rectified and filtered using a Half-Gaussian filter given by

$$p(EMG|x) = 2 \times \frac{\exp\left(-\frac{EMG^2}{2x^2}\right)}{\sqrt{2\pi x^2}}, \quad (1)$$

where $p(EMG|x)$ is a conditional probability density function, x is a latent driving signal and EMG is the rectified signal from the sensors.

The preprocessed sEMG data from the three sensors are fused using a sensor fusion algorithm to facilitate the extraction of the best finger force estimates. Sensor fusion is accomplished in the frequency domain using a simple elitism based Genetic Algorithm (GA). The SI method is used to identify the dynamical relationship between the sEMG data from the three sensors and the corresponding finger force. In this fusion algorithm, Output Error (OE) models are used to achieve the SI. The OE models are constructed for each individual data set. The OE model structure is given as follows.

$$y(t) = \frac{B(q)}{F(q)} u(t - nk) + e(t), \tag{2}$$

Where B and F are the polynomials, q is shift operator, $e(t)$ is output error, $y(t)$ is system output, u is input, nk is the system delay and t is time index.

Using the three resulting OE models and the fusion algorithm given by [6], a corresponding continuous-time model is constructed as given by the transfer function as

$$G(s) = \frac{B(s)}{F(s)} = \frac{b_{nb}s^{(nb-1)}b_{nb-1}s^{(nb-2)} + \cdots + b_1}{s^{nf} + f_{nf}s^{nf-1} + \cdots + f_1}, \tag{3}$$

Similar to the discrete-time case , nb and nf determine the orders of the numerator and denominator. For multi-input systems, nb and nf are row vectors. b, f are the coefficients of the numerator and denominator polynomials respectively.

A MISO transfer function is constructed based on the poles of three individual OE models corresponding to each sensor. GA is used to find the corresponding zeros. The search area is limited to the unit circle, because a discrete time model is used (and the resulting MISO model is decreased to minimum phase). The number of zeros is at most the number of poles. The number of potential zeros is set to the order of the corresponding denominator. The square error of the resulting MISO system $H(s)$ (see Appendix) and the recorded force signal is set as an objective function. The objective function f is constructed as follows,

$$f = \int_{t_0}^{t_f} (\hat{Y}(t) - Y(t)^2 dt = \int_{t_0}^{t_f} \varphi^2(t) dt, \tag{3}$$

where t_0 and t_f are the initial and final time values, $\widehat{Y}(t)$ is the fusion model estimated force and $Y(t)$ is the actual force from the FSR.

The MISO system $H(s)$ is constructed as follows,

$$H(s) = \begin{pmatrix} \frac{Z_{1,1}s^n + Z_{1,2}s^{n-1} + \cdots Z_{1,n+1}}{P_{1,1}s^n + P_{1,2}s^{n-1} + \cdots P_{1,n+1}} \\ \frac{Z_{2,1}s^n + Z_{2,2}s^{n-1} + \cdots Z_{2,n+1}}{P_{2,1}s^n + P_{2,2}s^{n-1} + \cdots P_{2,n+1}} \\ \frac{Z_{3,1}s^n + Z_{3,2}s^{n-1} + \cdots Z_{3,n+1}}{P_{3,1}s^n + P_{3,2}s^{n-1} + \cdots P_{3,n+1}} \end{pmatrix}, \tag{4}$$

where $Z's$ and $P's$ are the zeros and poles respectively of the individual transfer function and n is the order of the system.

Feeding the new data sets to the MISO transfer function ($H(s)$) results in an estimated fusion based force $\hat{Y}$.

IV. DYNAMICS OF PROSTHETIC HAND

The dynamic equations of motion for the hand are obtained from the Lagrangian approach as [8,9,10,11,12, 13]

$$\frac{d}{dt}\left(\frac{\partial \mathcal{L}}{\partial \dot{q}}\right) - \frac{\partial \mathcal{L}}{\partial q} = \tau \ , \tag{5}$$

where $\dot{q}$ and q represent the angular velocity and angle vectors of joints respectively; $\mathcal{L}$ is the Lagrangian; τ is the given torque vector at joints. The Lagrangian $\mathcal{L}$ is given as

$$\mathcal{L} = T - V, \tag{6}$$

where T and V are denoted as kinetic and potential energies respectively. Substituting (6) into (5), we get the following dynamic equations

$$M(q)\ddot{q} + C(q, \dot{q}) + G(q) = \tau, \tag{7}$$

where $M(q)$ describes the inertia matrix; $C(q, \dot{q})$ is the coriolis/centripetal vector and $G(q)$ is the gravity vector. (7) can be written as

$$M(q)\ddot{q} + N(q, \dot{q}) = \tau \ , \tag{8}$$

where $N(q, \dot{q}) = C(q, \dot{q}) + G(q)$ represents nonlinear terms.

Feedback linearization technique is used to convert the nonlinear dynamics represented by (8) into a linear state-variable system [8]. In order to obtain the alternative state-space equations of the dynamics, the position/velocity state $x(t)$ of the joint is defined as

$$x(t) = [q'(t)\ \dot{q}'(t)]' \ , \tag{9}$$

and rewriting (8) as,

$$\frac{d}{dt}\dot{q}(t) = -M^{-1}(q(t))[N(q(t), \dot{q}(t)) - \tau(t)] \tag{10}$$

Therefore, from (9) and (10), a linear system in Brunovsky canonical form is obtained and represented as

$$\dot{\mathrm{x}}(\mathrm{t}) = \begin{bmatrix} 0 & \mathrm{I} \\ 0 & 0 \end{bmatrix} \mathrm{x}(\mathrm{t}) + \begin{bmatrix} 0 \\ \mathrm{I} \end{bmatrix} \mathrm{u}(\mathrm{t}). \tag{11}$$

The control input vector $\mathrm{u}(t)$ given by

$$u(t) = -M^{-1}(q(t))\left[N(q(t), \dot{q}(t)) - \tau(t)\right]. \tag{12}$$

As the prosthetic hand is required to track the desired force profile $q_d(t)$ described under the reference force model, the tracking error $e(t)$ is defined as

$$e(t) = q_d(t) - q(t). \quad (13)$$

Here, $q_d(t)$ is the desired angle vector of the joints and can be obtained by the reference force model [6]; $q(t)$ is the actual angle vector of the joints. Differentiating (13) twice, we get,

$$\dot{e}(t) = \dot{q}_d(t) - \dot{q}(t)\ ,\ \ddot{e}(t) = \ddot{q}_d(t) - \ddot{q}(t). \quad (14)$$

Substituting (10) into (14) gives

$$\ddot{e}(t) = \ddot{q}_d(t) + M^{-1}(q(t))[N(q(t), \dot{q}(t)) - \tau(t)]. \quad (15)$$

From (15) the control function $u(t)$ can be defined as

$$u(t) = \ddot{q}_d(t) + M^{-1}(q(t))[N(q(t), \dot{q}(t)) - \tau(t)]. \quad (16)$$

This is often called the feedback linearization control law, rewriting (16) as,

$$\tau(t) = M(q(t))[\ddot{q}_d(t) - u(t) + N(q(t), \dot{q}(t))]. \quad (17)$$

Using (14) and (16), the state vector $x(t) = [e'(t)\dot{e}'(t)]'$, the state-space model can be represented as

$$\dot{x}(t) = \begin{bmatrix} 0 & I \\ 0 & 0 \end{bmatrix} x(t) + \begin{bmatrix} 0 \\ I \end{bmatrix} u(t). \quad (18)$$

Now, (18) is in the form of a linear system such as

$$\dot{x}(t) = Ax(t) + Bu(t)\ . \quad (19)$$

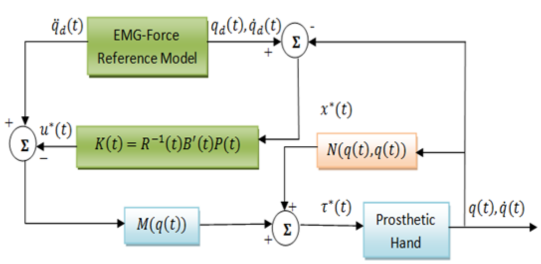

Fig. 1 Block Diagram of Optimal Controller for Prosthetic Hand.

OPTIMAL TRACKING

Figure 1 shows the block diagram representation of the finite-time linear quadratic optimal controller for the prosthetic hand. The objective of the controller is for the prosthetic hand finger to track optimally the force model.

For the linear system (19), the finite-time linear quadratic optimal control problem can be formulated by defining the performance index J [14] as

$$J = \frac{1}{2}\int_{t_0}^{t_f} [x'(t)\, Q(t)x(t) + u'(t)R(t)u(t)]\, dt \quad (20)$$

where $Q(t)$ is the error weighted matrix; and $R(t)$ is the control weighted matrix. The optimal control $u^*(t)$ is described by

$$u^*(t) = -R^{-1}(t)B'P(t)x^*(t) = -K(t)x^*(t). \quad (21)$$

where $K(t) = -R^{-1}(t)B'P(t)$ is called Kalman gain and $P(t)$, is the solution of the matrix differential Riccati equation (DRE)

$$\dot{P}(t) = -P(t)A - A'P(t) - Q(t) + P(t)BR^{-1}(t)B'P(t) \quad (22)$$

Satisfying the final condition

$$P(t = t_f) = 0. \quad (23)$$

Hence the optimal state x^* is the solution of

$$\dot{x}^*(t) = [A - BR^{-1}(t)B'P(t)]x^*(t). \quad (24)$$

Therefore, with the optimal control $u^*(t)$, the required torque $\tau^*(t)$ can be calculated by

$$\tau^*(t) = M(q(t))(\ddot{q}_d(t) - u^*(t)) + N(q(t), \dot{q}(t)). \quad (25)$$

The torque $\tau^*(t)$ is converted into force by

$$F_o(t) = \tau^*(t)/L, \quad (26)$$

where $F_o(t)$is the total force output of the index finger and L is the length of the finger. In this present work L is taken as 2.5 inches.

VI. RESULTS AND DISCUSSION

Figure 2 shows the fusion model force $\widehat{Y}(t)$ and the force output from the controller $F_o(t)$. It is evident that the optimal controller can track the changes in the force profile and follow the trends in reference force profile.

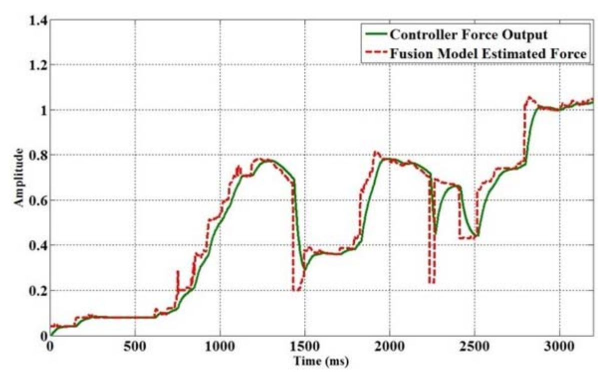

Fig. 2. Fusion Reference Model Force and Actual Force

Figure 3 shows the error between the model force $\widehat{Y}(t)$ and the force output from the controller $F_o(t)$ for two different sets of results shown in Figs. 2 and 4. This figure shows that the error converged to zero in a very short time and the error is hovering between zero throughout the time interval. In some instances the force output of the controller $F_o(t)$ cannot track the rapidly changing reference force profile during short intervals. The Pearson correlation coefficient (see Appendix) for the reference

$\hat{Y}(t)$ and controller output force $F_o(t)$ profile is 0.8714. Figure 4 shows the validation with a different reference force $\hat{Y}(t)$ profile and it yields 0.8707 correlation, thus showing good agreement between the reference model force and the actual force.

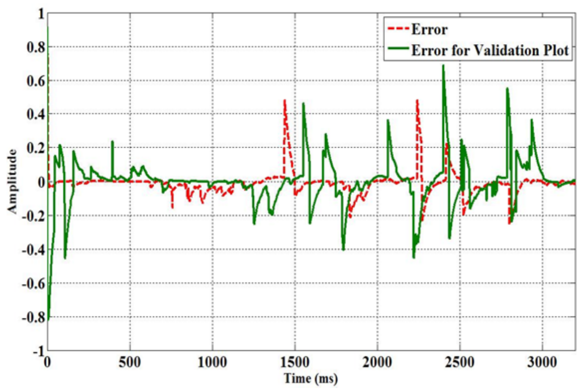

Fig. 3. Error between the Model Force and the Actual Force

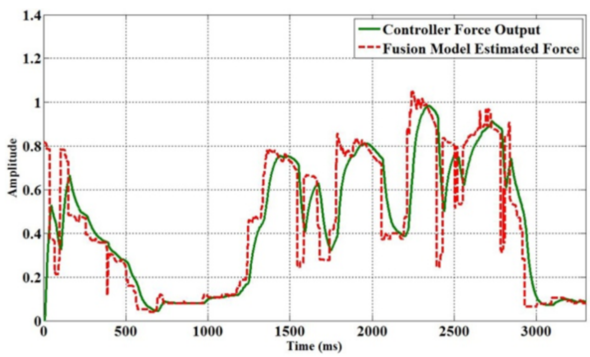

Fig. 4. Validation Plot

VII. Conclusion and Future Work

A fusion-based sEMG-force model was utilized to estimate the force profile that a prosthetic hand should track. This fusion enables to get better force estimates than the single sensor data. The dynamics of the hand was obtained and the controller for optimal tracking between the reference model and the hand was designed. The proposed design gives good performance when tested on a prosthetic hand, based on tracking a reference force profile. In future, we plan to implement this proposed control strategy on a micro controller for real time control. It would be interesting to implement both the force and position control using this control strategy. Finally, we plan to use the hand prototype with five fingers.

Appendix

The resulting MISO transfer function $H(s)$ is constructed as,

From u_1 to output,

$$\frac{s^8 - 3.843s^7 + 7.729s^6 - 10.78s^5 + 10.6s^4 - 7.417s^3 + 3.603s^2 - 0.9795s + 0.1192}{s^8 - 4.028s^7 + 6.325s^6 - 4.121s^5 - 1.545s^4 + 5.87s^3 - 5.433s^2 + 2.28s - 0.3496}$$

From u_2 to output,

$$\frac{s^8 - 4.339s^7 + 9.005s^6 - 12.42s^5 + 12.22s^4 - 8.117s^3 + 3.427s^2 - 0.9134\,s + 0.1424}{s^8 - 4.028\,s^7 + 6.325\,s^6 - 4.121\,s^5 - 1.545\,s^4 + 5.87\,s^3 - 5.433\,s^2 + 2.28\,s - 0.3496}$$

From u_3 to output,

$$\frac{s^8 - 3.522\,s^7 + 6.655\,s^6 - 8.864\,s^5 + 8.183\,s^4 - 5.365\,s^3 + 2.423\,s^2 - 0.557\,s + 0.09585}{s^8 - 4.028\,s^7 + 6.325\,s^6 - 4.121s^5 - 1.545\,s^4 + 5.87\,s^3 - 5.433\,s^2 + 2.28\,s - 0.3496}$$

where u_1, u_2, u_3 are the data from three sensors.

Pearson correlation coefficient is given by,

$$\rho_{X,Y} = corr(X,Y) = \frac{cov(X,Y)}{\sigma_X \sigma_Y} = \frac{E[(X-\mu_X)(Y-\mu_Y)]}{\sigma_X \sigma_Y}$$

Where X, Y are Random Variables, μ_X and μ_Y are expected values, σ_X, σ_Y are standard deviations respectively. E is expected value operator.

Acknowledgment

This research was sponsored by the US Department of the Army, under the award number W81XWH-10-1-0128 awarded and administered by the U.S. Army Medical Research Acquisition Activity, 820 Chandler Street, Fort Detrick MD 21702-5014. The information does not necessarily reflect the position or the policy of the Government, and no official endorsement should be inferred. For purposes of this article, information includes news releases, articles, manuscripts, brochures, advertisements, still and motion pictures, speeches, trade association proceedings, etc. Further, the technical help from Dr. Cheng-Hung Chen, Mr. Amir Fassih and Mr. Parmod Kumar is greatly appreciated.

References

[1] "Aca News: National Limb Loss Awareness Month" 2011. Retrieved from http://www.bocusa.org/aca-news-national-limb-loss-awareness-month
[2] D.S. Naidu and C.-H. Chen, "*Control Strategies for Smart Prosthetic Hand Technology: An Overview*", Book Chapter 14, to appear in a book titled, Distributed Diagnosis and Home Healthcare (D2H2): Volume 2, American Scientific Publishers, CA, January 2011.
[3] Zinn M, Roth B, Khatib O, and Salisbury JK, "*A new actuation approach for human friendly robot design*," *Int J Robot Res.* 2004; 23(4-5), pp. 379-398.
[4] Heinzmann J, and Zelinsky J, "*A safe-control paradigm for human-robot interaction,*" J Intell Robot Syst. 1999; 25(4): pp. 295-310.
[5] Kandel E.R. and Schartz J.H., "*Principles of Neural Science,*" Elsevier/North-Holland, New York, 1981.
[6] Potluri C., Kumar P., Anugolu M., Urfer A., Chiu S., Naidu D.S., and Schoen M, *"Frequency Domain Surface EMG Sensor Fusion for Estimating Finger Forces,"* 32nd Annual International Conference of the IEEE Engineering in Medicine and Biology Society, Buenos Aires, Argentina, August 31 - September 4, 2010.
[7] http://www.isek-online.org/standards_emg.html.
[8] F.L.Lewis, D.M.Dawson, and C.T. Abdallah, "*Robot Manipulators Control: Second Edition, Revised and Expanded"*, New York, NY: Marcel Dekker, Inc., 2004.
[9] B.Siciliano, L.Sciavicco, L. Villani, and G. Oriolo, "*Robotics: Modelling, Planning and Control"*. London, UK: Springer-verlag, 2009.
[10] C-H. Chen, *"Hybrid Control Strategies for Smart Prosthetic Hand*", Ph.D dissertation, Measurement and Control Engineering, Idaho State University, May 2009.
[11] R. Kelly, V. Santidanez, and A. Loria, "*Control of Robot Manipulators in Joint Space*", New York, USA, Springer, 2005.
[12] R.N. Jazar, "*Theory of Applied Robotics, Kinematics, Dynamics, and Control"*, New York, USA, Springer 2007.
[13] C-H Chen and D.S.Naidu, *"Optimal Control Strategy For Two-Fingered Smart Prosthetic Hand*", Proceedings of the IASTED International Conference Robotics and Applications (RA 2010), November 1-3, Cambridge, Massachusetts, USA, 2010.
[14] D. Naidu, "*Optimal Control Systems*", Boca Raton, FL, CRC Press, 2003.